Agricultural and Forest Meteorology 336 (2023) 109479

Contents lists available at ScienceDirect

Agricultural and Forest Meteorology

journal homepage: www.elsevier.com/locate/agrformet

Review

Refinements of equations for the temperature-wind covariance in Massman and Lee (2002)

Hanshu Wang[a], Yaoming Ma[a,b,c,d,e,f,*], William J. Massman[g], John M. Frank[g]

[a] College of Atmospheric Sciences, Lanzhou University, Lanzhou 730000, China
[b] State Key Laboratory of Tibetan Plateau Earth System, Resources and Environment (TPESRE), Institute of Tibetan Plateau Research, Chinese Academy of Sciences, Beijing 100101, China
[c] College of Earth and Planetary Sciences, University of Chinese Academy of Sciences, Beijing 100049, China
[d] National Observation and Research Station for Qomolongma Special Atmospheric Processes and Environmental Changes, Dingri 858200, China
[e] Kathmandu Center of Research and Education, Chinese Academy of Sciences, Beijing 100101, China
[f] China-Pakistan Joint Research Center on Earth Sciences, Chinese Academy of Sciences, Islamabad 45320, Pakistan
[g] USDA Forest Service, Rocky Mountain Research Station, Fort Collins, CO, USA

ARTICLE INFO

Keywords:
Temperature-wind covariance
Sonic temperature
Error correction for equations
Quantitative estimation

ABSTRACT

We present refinements for equations describing the temperature-wind covariance ($\overline{v'T_a'}$) reported by Massman and Lee (2002); namely, Eqs. (B.24), (B.25), and (B.28) in its Appendix B. The purpose of these equations is to express the wind covariance of air temperature (T_a) in terms of sonic temperature (T_s), as a sonic anemometer directly measures the latter rather than the former. Results of the derivations are summarized in Tables 1 and 2, and these refinements have been quantified using data from the Glacier Lakes Ecosystem Experiments Site (GLEES).

1. Introduction

The eddy covariance (EC) method serves as a mainstream way to measure gas fluxes in and out of an ecosystem (Burba 2022), which plays a fundamental role in quantifying the surface-air exchange within the atmospheric boundary layer. The validity of the EC method is based on a series of theoretical works, among which Webb et al. (1980) (hereinafter WPL80) is recognized as a milestone by the flux community. WPL80 proposed the original version of the WPL theory. The historical evolution of this theory has been summarized in Fuehrer and Friehe (2002) and Lee and Massman (2011).

WPL80 derived the "density effect corrections" under the assumptions of steady state, horizontal homogeneity (which means only the vertical components remain) and a zero mean vertical flux of the dry air component. The last assumption, defined as the "governing constraint" in WPL80, has become a controversial scientific question especially in the past two decades. Fundamental works since then discarded the assumption of a zero dry air flux, and extended the result of WPL80 to non-steady state or horizontally heterogeneous conditions using the constraint of mass conservation equations, such as Paw U et al. (2000), Massman and Lee (2002), Leuning (2004, 2007), Lee and Massman (2011) and Gu et al. (2012). Nevertheless, the validity of WPL80 under steady state, horizontally homogeneous conditions is still proven by these works. Recently, Kowalski et al. (2021) proposed a new set of definitions to partition the total flux into turbulent and non-turbulent transports considering the conservation of momentum, but still verified the overall correctness of the total flux after WPL corrections.

Among these works revising WPL80, Massman and Lee (2002), is the first one to provide basic equations for the eddy covariance method in a 3D format based on mass conservation. The 3D equations proposed by Massman and Lee (2002) (mostly in its Appendix B) are comprehensive in all dimensions (x, y, z, t), with detailed derivations and succinct expressions. It serves as an instructive work to demonstrate the EC basic principles, and therefore has reasonably gained a high number of citations (554 citations till March 29, 2023; 10.1016/S0168–1923(02)00105–3).

However, there are inaccuracies in Eqs. (B.24), (B.25), and (B.28) in Appendix B of Massman and Lee (2002) that have not been reported by the scientific community before. These three equations describe the relationship between the ambient air temperature (T_a) and the sonic temperature (T_s), with the latter being directly measured by a sonic anemometer. The aim of these equations is to calculate the

* Corresponding author at: College of Atmospheric Sciences, Lanzhou University, Lanzhou 730000, China.
E-mail address: ymma@itpcas.ac.cn (Y. Ma).

https://doi.org/10.1016/j.agrformet.2023.109479
Received 22 December 2022; Received in revised form 18 April 2023; Accepted 20 April 2023
Available online 5 May 2023
0168-1923/© 2023 The Authors. Published by Elsevier B.V. This is an open access article under the CC BY license (http://creativecommons.org/licenses/by/4.0/).

temperature-wind covariance ($\overline{v'T'_a}$, termed as "temperature flux" in Massman and Lee (2002)) with the covariance between the measured sonic temperature and the wind speed ($\overline{v'T'_s}$).

This paper corrects the inaccuracies in these equations. Section 2 describes the typo in Eq. (B.24) and the resulting errors in Eqs. (B.25) and (B.28), and proposes the correct equations with detailed derivations. Section 3 summarizes the theoretical results in Section 2. Section 4 presents quantitative estimations for the errors in these equations using data from the Glacier Lakes Ecosystem Experiments Site (GLEES), an AmeriFlux site in southeastern Wyoming, USA (Burns et al., 2021; Frank and Massman, 2021).

2. Corrections to Massman And Lee (2002)

2.1. Eq. (B.24)

Eq. (B.24) of Massman and Lee (2002) was originally written as follows:

$$T'_s = T'_a(1+\overline{\sigma}_v) + \overline{\sigma}_v \overline{T}_a \left(\frac{\rho'_v}{\overline{\rho}_v} - \frac{p'_a}{\overline{p}_a} \right) \tag{B.24}$$

There exists a typographical error in Eq. (B.24), which is that ρ_v (density of water vapor) appears instead of p_v (partial pressure of water vapor). We will prove this claim in the following derivation.

Massman and Lee (2002) defined the sonic temperature T_s as:

$$T_s = T_a\left(1+0.32\frac{p_v}{p_a}\right) = T_a(1+\sigma_v) \tag{1}$$

in which:

$$\sigma_v \equiv 0.32\frac{p_v}{p_a} \tag{2}$$

All symbols used here have the same meanings as those in Massman and Lee (2002): T_a is the ambient air temperature, p_a is the ambient air pressure (i.e. air pressure of the total moist air), and p_v is the partial pressure of water vapor.

We applied Reynolds decomposition to Eqs. (1) and (2), where we ignore the covariance term ($\overline{\sigma'_v p'_a}$) and the second-order fluctuation term ($\sigma'_v p'_a/\overline{\sigma}_v\overline{p}_a$) as Massman and Lee (2002). This is equivalent to a first-order Taylor expansion, where a logarithm is applied to Eqs. (1) and (2) as the first step of the expansion (see Appendix). As a result, we produced the means and fluctuations of σ_v and T_s. Overbars denote mean values and primes refer to fluctuations.

For $\overline{\sigma}_v$:

$$\overline{\sigma}_v = 0.32\frac{\overline{p}_v}{\overline{p}_a} = 0.32\frac{\overline{p}_v}{\overline{p}_d+\overline{p}_v} = 0.32\frac{\overline{\chi}_v}{1+\overline{\chi}_v} \tag{3}$$

where $\overline{p}_a = \overline{p}_d + \overline{p}_v$ and $\overline{\chi}_v = \overline{p}_v/\overline{p}_d$. Here $\overline{p}_d$ is the mean partial pressure of the dry air component (including CO_2, as in Massman and Lee (2002)), and $\overline{\chi}_v$ is the mean mole fraction of water vapor relative to dry air.

For σ'_v:

$$\frac{\sigma'_v}{\overline{\sigma}_v} = \frac{p'_v}{\overline{p}_v} - \frac{p'_a}{\overline{p}_a} \tag{4}$$

or

$$\sigma'_v = \overline{\sigma}_v\left(\frac{p'_v}{\overline{p}_v} - \frac{p'_a}{\overline{p}_a}\right) \tag{4a}$$

For T_s:

$$\overline{T}_s = \overline{T}_a(1+\overline{\sigma}_v) \tag{5}$$

and

$$\frac{T'_s}{\overline{T}_s} = \frac{T'_a}{\overline{T}_a} + \frac{\sigma'_v}{(1+\overline{\sigma}_v)} = \frac{T'_a}{\overline{T}_a} + \frac{\overline{\sigma}_v}{1+\overline{\sigma}_v}\left(\frac{p'_v}{\overline{p}_v} - \frac{p'_a}{\overline{p}_a}\right) \tag{6}$$

When considering Eq. (5), this becomes:

$$T'_s = T'_a(1+\overline{\sigma}_v) + \overline{\sigma}_v\overline{T}_a\left(\frac{p'_v}{\overline{p}_v} - \frac{p'_a}{\overline{p}_a}\right) \tag{7}$$

Eq. (7), which is equivalent to Eq. (6), is the correct version of Eq. (B.24) in Massman and Lee (2002). Examination of this shows the typo in Eq. (B.24): the p_v term in Eq. (7) was wrongly replaced with ρ_v. The correct way to express p_v with ρ_v in Eqs. (6) or (7) is described below.

What we need is the Ideal Gas Law of water vapor:

$$p_v = \frac{\rho_v}{m_v}RT_a \tag{8}$$

where m_v is the molecular mass of water vapor and R is the universal gas constant. Conducting Reynolds decomposition on Eq. (8), we get:

$$\frac{p'_v}{\overline{p}_v} = \frac{T'_a}{\overline{T}_a} + \frac{\rho'_v}{\overline{\rho}_v} \tag{9}$$

Then, by substituting Eq. (9) into Eqs. (6) or (7) to eliminate p_v, we get:

$$\frac{T'_s}{\overline{T}_s} = \frac{T'_a}{\overline{T}_a} + \frac{\overline{\sigma}_v}{1+\overline{\sigma}_v}\left(\frac{T'_a}{\overline{T}_a} + \frac{\rho'_v}{\overline{\rho}_v} - \frac{p'_a}{\overline{p}_a}\right) = \frac{1+2\overline{\sigma}_v}{1+\overline{\sigma}_v}\frac{T'_a}{\overline{T}_a} + \frac{\overline{\sigma}_v}{1+\overline{\sigma}_v}\left(\frac{\rho'_v}{\overline{\rho}_v} - \frac{p'_a}{\overline{p}_a}\right) \tag{10}$$

or

$$T'_s = T'_a(1+2\overline{\sigma}_v) + \overline{\sigma}_v\overline{T}_a\left(\frac{\rho'_v}{\overline{\rho}_v} - \frac{p'_a}{\overline{p}_a}\right) \tag{11}$$

Here, the p_v in Eq. (7) has been replaced with ρ_v in the correct manner. It should be noted that Eqs. (10) and (11) are equivalent to Eqs. (6) and (7), and all four correct the error in Eq. (B.24). When ρ_v is used instead of p_v, the difference between our Eq. (11) and the original Eq. (B.24) of Massman and Lee (2002) lies in the parameters given for T'_a, namely $(1+2\overline{\sigma}_v)$ instead of $(1+\overline{\sigma}_v)$.

2.2. Eq. (B.25)

In this sub-section, we will firstly present the procedures to derive Eq. (B.25) from Eq. (B.24), which were not demonstrated with enough details in Massman and Lee (2002). Then we will prove that Eq. (B.25) is incorrect based on the analyses of these procedures. Finally, we will derive the correct version of Eq. (B.25) and compare it with the original one.

The original version of Eq. (B.25) presented in Massman and Lee (2002) is

$$\overline{v'T'_a} = \frac{\overline{v'T'_s}}{1+\overline{\sigma}_v} - \frac{\overline{\sigma}_v}{1+\overline{\sigma}_v}\overline{T}_a\left(\frac{\overline{v'\rho'_v}^F}{\overline{\rho}_v} - \frac{\overline{v'p'_a}}{\overline{p}_a}\right) \tag{B.25}$$

Eq. (B.25) can be readily deduced from Eq. (B.24) in two steps. First we derive "the flux version of Eq. (B.24)" as:

$$\overline{v'T'_a} = \frac{\overline{v'T'_s}}{1+\overline{\sigma}_v} - \frac{\overline{\sigma}_v}{1+\overline{\sigma}_v}\overline{T}_a\left(\frac{\overline{v'\rho'_v}}{\overline{\rho}_v} - \frac{\overline{v'p'_a}}{\overline{p}_a}\right) \tag{B.24F}$$

It can be obtained by singling out T'_a, multiplying with v' and applying the Reynolds averaging for Eq. (B.24). Second we replace $\overline{v'\rho'_v}$ with $\overline{v'\rho'_v}^F$ in Eq. (B.24$_F$). Then Eq. (B.25) is produced.

However, as we have noted in the last section, Eq. (B.24) is incorrect. So Eq. (B.25) is also flawed since it is derived from Eq. (B.24).

Additionally, it is wrong to replace $\overline{v'\rho'_v}$ with $\overline{v'\rho'_v}^F$ because

$\overline{v'\rho_v'} \neq \overline{v'\rho_v'}^{\mathrm{F}}$. According to Massman and Lee (2002), $\overline{v'\rho_v'}^{\mathrm{F}}$ represents the "complete flux" of water vapor including the WPL corrections. It can be written specifically as:

$$\overline{v'\rho_v'}^{\mathrm{F}} = \overline{v'\rho_v'} - \overline{\omega}_v \overline{v'\rho_d'} \tag{12a}$$

or

$$\frac{\overline{v'\rho_v'}^{\mathrm{F}}}{\overline{\rho}_v} = (1+\overline{\chi}_v)\left(\frac{\overline{v'\rho_v'}}{\overline{\rho}_v} + \frac{\overline{v'T_a'}}{\overline{T}_a} - \frac{\overline{v'p_a'}}{\overline{p}_a}\right) \tag{12b}$$

in which ρ_d is the density of dry air ($\rho_d = \rho_a - \rho_v$) and $\overline{\omega}_v = \overline{\rho}_v / \overline{\rho}_d$ is the mean mixing ratio of water vapor. Unless the last term in Eq. (12a) equals zero, it follows that $\overline{v'\rho_v'} \neq \overline{v'\rho_v'}^{\mathrm{F}}$. Thus, replacing $\overline{v'\rho_v'}$ with $\overline{v'\rho_v'}^{\mathrm{F}}$ is mathematically incorrect. It is also unnecessary to do so, given that our final goal is to express $\overline{v'T_a'}$ in relation to $\overline{v'\rho_v'}$ (the raw flux of water vapor) rather than $\overline{v'\rho_v'}^{\mathrm{F}}$, as pointed out by Eq. (B.28) in Massman and Lee (2002):

$$\frac{\overline{v'T_a'}}{\overline{T}_a} = \left[\frac{1}{1+\delta_{oc}\overline{\lambda}_v}\right]\frac{\overline{v'T_s'}}{\overline{T}_s} - \left[\frac{\overline{\alpha}_v(1+\overline{\chi}_v)}{1+\delta_{oc}\overline{\lambda}_v}\right]\frac{\overline{v'\rho_v'}}{\overline{\rho}_d} + \left[\frac{\overline{\beta}_v(2+\overline{\chi}_v)}{1+\delta_{oc}\overline{\lambda}_v}\right]\frac{\overline{v'p_a'}}{\overline{p}_a} \tag{B.28}$$

As such, Eq. (B.25) must be incorrect.

The correct version of Eq. (B.25) can easily be derived from Eq. (11) by following the same mathematical procedures to derive Eq. (B.25) from Eq. (B.24) described at the beginning of this sub-section, without substituting $\overline{v'\rho_v'}$ with $\overline{v'\rho_v'}^{\mathrm{F}}$:

$$\overline{v'T_a'} = \frac{\overline{v'T_s'}}{1+2\overline{\sigma}_v} - \frac{\overline{\sigma}_v}{1+2\overline{\sigma}_v}\overline{T}_a\left(\frac{\overline{v'\rho_v'}}{\overline{\rho}_v} - \frac{\overline{v'p_a'}}{\overline{p}_a}\right) \tag{13}$$

Eq. (13) shown here is the correct version of Eq. (B.25). Comparing Eq. (13) and Eq. (B.25) we can see that (i) the typographical error in Eq. (B.24) creates a difference between the denominators $(1+2\overline{\sigma}_v)$ and $(1+\overline{\sigma}_v)$; (ii) the mistake of replacing $\overline{v'\rho_v'}$ with $\overline{v'\rho_v'}^{\mathrm{F}}$ is also shown clearly.

2.3. Eq. (B.28)

Eq. (B.28) was directly derived from Eq. (B.25); however, since the latter is wrong, Eq. (B.28) must also be incorrect.

In order to keep the equation concise, we do not introduce additional parameters, such as $\overline{\alpha}_v$, $\overline{\beta}_v$, and $\overline{\lambda}_v$, as performed by Massman and Lee (2002). Instead, we express the revised version of Eq. (B.28) using only $\overline{\sigma}_v$ or $\overline{\chi}_v$.

The purpose of Eq. (B.28) was to express the wind covariance of air temperature ($\overline{v'T_a'}/\overline{T}_a$) with that of sonic temperature ($\overline{v'T_s'}/\overline{T}_s$), given that sonic anemometers directly measure T_s rather than T_a. Eq. (B.24) and (B.25) are intermediate steps towards Eq. (B.28). By multiplying Eq. (13) with $1/\overline{T}_a$ and then employing Eq. (5), the correct version of Eq. (B.28) can be produced, which directly satisfies this purpose:

$$\frac{\overline{v'T_a'}}{\overline{T}_a} = \frac{1+\overline{\sigma}_v}{1+2\overline{\sigma}_v}\frac{\overline{v'T_s'}}{\overline{T}_s} - \frac{\overline{\sigma}_v}{1+2\overline{\sigma}_v}\left(\frac{\overline{v'\rho_v'}}{\overline{\rho}_v} - \frac{\overline{v'p_a'}}{\overline{p}_a}\right) \tag{14a}$$

When considering Eq. (3) to replace the parameter of $\overline{\sigma}_v$ with $\overline{\chi}_v$, we obtain the following:

$$\frac{\overline{v'T_a'}}{\overline{T}_a} = \frac{1+1.32\overline{\chi}_v}{1+1.64\overline{\chi}_v}\frac{\overline{v'T_s'}}{\overline{T}_s} - \frac{0.32\overline{\chi}_v}{1+1.64\overline{\chi}_v}\left(\frac{\overline{v'\rho_v'}}{\overline{\rho}_v} - \frac{\overline{v'p_a'}}{\overline{p}_a}\right) \tag{14b}$$

Eqs. (14a) or (14b) are both correct forms of Eq. (B.28).

To simplify the coefficients, we can rewrite Eqs. (14a) and (14b) as:

$$\frac{\overline{v'T_a'}}{\overline{T}_a} = \frac{\overline{v'T_s'}}{\overline{T}_s} - \overline{\Gamma}_v\left(\frac{\overline{v'T_s'}}{\overline{T}_s} + \frac{\overline{v'\rho_v'}}{\overline{\rho}_v} - \frac{\overline{v'p_a'}}{\overline{p}_a}\right) \tag{15}$$

where

$$\overline{\Gamma}_v = \frac{\overline{\sigma}_v}{1+2\overline{\sigma}_v} = \frac{0.32\overline{\chi}_v}{1+1.64\overline{\chi}_v} \tag{15a}$$

We can conduct a preliminary estimation for Eqs. (15) and (15a) according to Eqs. (18a)–(18d) in Section 4:

$$\overline{\Gamma}_v \sim \overline{\chi}_v \sim 10^{-3} \tag{15b}$$

and

$$\frac{\overline{v'T_a'}}{\overline{T}_a} \approx \frac{\overline{v'T_s'}}{\overline{T}_s} \tag{15c}$$

Eqs. (14a), 14b) and ((15) are more succinct than the original Eq. (B.28) in Massman and Lee (2002).

3. Comparison of the original and corrected versions of the three equations

In Section 2, we corrected the typographical error in Eq, (B.24) of Massman and Lee (2002) and the corresponding errors in Eqs. (B.25) and (B.28). To summarize, we list the original and corrected versions of Eq. (B.24), (B.25), and (B.28) in Table 1. The formulae showing the absolute errors of the original versions are listed in the "Original Minus Corrected" column of Table 2, but these original versions of equations have been slightly modified before subtraction to show the T_a terms on the left-hand side for several reasons below.

As pointed out in Section 2.3, the purpose of these three equations was to calculate the wind covariance of T_a in terms of T_s, because sonic anemometers directly measure the latter rather than the former. Further, calculating the net ecosystem exchange (NEE) of a particular trace gas component (c) requires $\overline{v'T_a'}/\overline{T}_a$ more directly than $\overline{v'T_a'}$, as shown by the Eq. (1) in Burns et al. (2021) (horizontal exchanges ignored):

$$\mathrm{NEE} = \int_0^h \frac{\partial\overline{\rho}_c}{\partial t}dz + \overline{w'\rho_c'} - \overline{\rho}_c(1+\overline{\chi}_v)\frac{\overline{w'p_a'}}{\overline{p}_a} + \overline{\rho}_c(1+\overline{\chi}_v)\frac{\overline{w'T_a'}}{\overline{T}_a} + \mu_v\frac{\overline{\rho}_c}{\overline{\rho}_d}\overline{w'\rho_v'} \tag{16}$$

where h is the measurement height, $\overline{\rho}_c$ the mean density of component c, w the vertical velocity, and μ_v the ratio of the molecular weight of dry air to that of water vapor.

For these reasons, we rearrange the equations to show $T_a'/\overline{T}_a$ or $\overline{v'T_a'}/\overline{T}_a$ on the left-hand side and other terms on the right-hand side, as shown in Table 2. We also note that we choose an open-path system for comparison, such that $\delta_{oc} = 1$. Additional parameters used in these equations are summarized as follows:

$$\overline{\beta}_v = \frac{\overline{\sigma}_v}{1+\overline{\sigma}_v} = \frac{0.32\overline{\chi}_v}{1+1.32\overline{\chi}_v} \tag{17a}$$

$$\overline{\lambda}_v = \overline{\beta}_v(1+\overline{\chi}_v) \tag{17b}$$

$$\overline{\alpha}_v = \overline{\beta}_v\frac{\overline{\rho}_d}{\overline{\rho}_v} \tag{17c}$$

$$\delta_{oc} = \begin{cases} 1, & \textit{open path IRGA} \\ 0, & \textit{closed path IRGA} \end{cases} \tag{17d}$$

4. Quantitative estimations of the errors of the original equations

4.1. An overview of the GLEES dataset

Eddy covariance data from the GLEES site (Frank and Massman,

Table 1
Summary of the original and corrected versions of Eqs. (B.24), (B.25), and (B.28) in Massman and Lee (2002).

Eq.	Original	Corrected
(B.24)	$T_s' = T_a'(1+\overline{\sigma}_v) + \overline{\sigma}_v\overline{T}_a\left(\frac{\rho_v'}{\overline{\rho}_v} - \frac{p_a'}{\overline{p}_a}\right)$	$T_s' = T_a'(1+\overline{\sigma}_v) + \overline{\sigma}_v\overline{T}_a\left(\frac{p_v'}{\overline{p}_v} - \frac{p_a'}{\overline{p}_a}\right)$ (7) or $T_s' = T_a'(1+2\overline{\sigma}_v) + \overline{\sigma}_v\overline{T}_a\left(\frac{\rho_v'}{\overline{\rho}_v} - \frac{p_a'}{\overline{p}_a}\right)$ (11)
(B.25)	$\overline{v'T_a'} = \frac{\overline{v'T_s'}}{1+\overline{\sigma}_v} - \frac{\overline{\sigma}_v}{1+\overline{\sigma}_v}\overline{T}_a\left(\frac{\overline{v'\rho_v'}^{F}}{\overline{\rho}_v} - \frac{\overline{v'p_a'}}{\overline{p}_a}\right)$	$\overline{v'T_a'} = \frac{\overline{v'T_s'}}{1+2\overline{\sigma}_v} - \frac{\overline{\sigma}_v}{1+2\overline{\sigma}_v}\overline{T}_a\left(\frac{\overline{v'\rho_v'}}{\overline{\rho}_v} - \frac{\overline{v'p_a'}}{\overline{p}_a}\right)$ (13)
(B.28)	$\frac{\overline{v'T_a'}}{\overline{T}_a} = \left[\frac{1}{1+\delta_{oc}\overline{\lambda}_v}\right]\frac{\overline{v'T_s'}}{\overline{T}_s} - \left[\frac{\overline{\alpha}_v(1+\overline{\chi}_v)}{1+\delta_{oc}\overline{\lambda}_v}\right]\frac{\overline{v'\rho_v'}}{\overline{\rho}_d} + \left[\frac{\overline{\beta}_v(2+\overline{\chi}_v)}{1+\delta_{oc}\overline{\lambda}_v}\right]\frac{\overline{v'p_a'}}{\overline{p}_a}$	$\frac{\overline{v'T_a'}}{\overline{T}_a} = \frac{1+\overline{\sigma}_v}{1+2\overline{\sigma}_v}\frac{\overline{v'T_s'}}{\overline{T}_s} - \frac{\overline{\sigma}_v}{1+2\overline{\sigma}_v}\left(\frac{\overline{v'\rho_v'}}{\overline{\rho}_v} - \frac{\overline{v'p_a'}}{\overline{p}_a}\right)$ (14a) or $\frac{\overline{v'T_a'}}{\overline{T}_a} = \frac{\overline{v'T_s'}}{\overline{T}_s} - \overline{\Gamma}_v\left(\frac{\overline{v'T_s'}}{\overline{T}_s} + \frac{\overline{v'\rho_v'}}{\overline{\rho}_v} - \frac{\overline{v'p_a'}}{\overline{p}_a}\right)$ (15)

Table 2
Comparison of the original and corrected versions of Eqs. (B.24), (B.25), and (B.28) in Massman and Lee (2002) for open-path systems. In each equation, the T_a term is situated on the left-hand side.

Eq.	Original	Corrected	Original Minus Corrected
(B.24)	$\frac{T_a'}{\overline{T}_a} = \frac{T_s'}{\overline{T}_s} - \frac{\overline{\sigma}_v}{1+\overline{\sigma}_v}\left(\frac{\rho_v'}{\overline{\rho}_v} - \frac{p_a'}{\overline{p}_a}\right)$	$\frac{T_a'}{\overline{T}_a} = \frac{1+\overline{\sigma}_v}{1+2\overline{\sigma}_v}\frac{T_s'}{\overline{T}_s} - \frac{\overline{\sigma}_v}{1+2\overline{\sigma}_v}\left(\frac{\rho_v'}{\overline{\rho}_v} - \frac{p_a'}{\overline{p}_a}\right)$	$\Delta\left(\frac{T_a'}{\overline{T}_a}\right) = \frac{\overline{\sigma}_v}{1+2\overline{\sigma}_v}\frac{T_s'}{\overline{T}_s} - \frac{\overline{\sigma}_v}{1+2\overline{\sigma}_v}\frac{\overline{\sigma}_v}{1+\overline{\sigma}_v}\left(\frac{\rho_v'}{\overline{\rho}_v} - \frac{p_a'}{\overline{p}_a}\right)$
(B.25)	$\frac{\overline{v'T_a'}}{\overline{T}_a} = \frac{\overline{v'T_s'}}{\overline{T}_s} - \frac{\overline{\sigma}_v}{1+\overline{\sigma}_v}\left(\frac{\overline{v'\rho_v'}^{F}}{\overline{\rho}_v} - \frac{\overline{v'p_a'}}{\overline{p}_a}\right)$	$\frac{\overline{v'T_a'}}{\overline{T}_a} = \frac{1+\overline{\sigma}_v}{1+2\overline{\sigma}_v}\frac{\overline{v'T_s'}}{\overline{T}_s} - \frac{\overline{\sigma}_v}{1+2\overline{\sigma}_v}\left(\frac{\overline{v'\rho_v'}}{\overline{\rho}_v} - \frac{\overline{v'p_a'}}{\overline{p}_a}\right)$	$\Delta\left(\frac{\overline{v'T_a'}}{\overline{T}_a}\right) = \frac{\overline{\sigma}_v}{1+2\overline{\sigma}_v}\frac{\overline{v'T_s'}}{\overline{T}_s} + \frac{\overline{\sigma}_v}{1+2\overline{\sigma}_v}\frac{\overline{v'\rho_v'}}{\overline{\rho}_v} - \frac{\overline{\sigma}_v}{1+\overline{\sigma}_v}\frac{\overline{v'\rho_v'}^{F}}{\overline{\rho}_v} + \frac{\overline{\sigma}_v}{1+2\overline{\sigma}_v}\frac{\overline{\sigma}_v}{1+\overline{\sigma}_v}\frac{\overline{v'p_a'}}{\overline{p}_a}$
(B.28)	$\frac{\overline{v'T_a'}}{\overline{T}_a} = \frac{\overline{v'T_s'}}{\overline{T}_s} - \frac{\overline{\lambda}_v}{1+\overline{\lambda}_v}\left(\frac{\overline{v'T_s'}}{\overline{T}_s} + \frac{\overline{v'\rho_v'}}{\overline{\rho}_v}\right) + \left[\frac{\overline{\beta}_v(2+\overline{\chi}_v)}{1+\overline{\lambda}_v}\right]\frac{\overline{v'p_a'}}{\overline{p}_a}$	$\frac{\overline{v'T_a'}}{\overline{T}_a} = \frac{\overline{v'T_s'}}{\overline{T}_s} - \frac{\overline{\sigma}_v}{1+2\overline{\sigma}_v}\left(\frac{\overline{v'T_s'}}{\overline{T}_s} + \frac{\overline{v'\rho_v'}}{\overline{\rho}_v} - \frac{\overline{v'p_a'}}{\overline{p}_a}\right)$	$\Delta\left(\frac{\overline{v'T_a'}}{\overline{T}_a}\right) = \frac{0.32\overline{\chi}_v}{(1+1.64\overline{\chi}_v)(1+1.64\overline{\chi}_v+0.32\overline{\chi}_v^2)}\left[-\overline{\chi}_v(1+1.32\overline{\chi}_v)\left(\frac{\overline{v'T_s'}}{\overline{T}_s} + \frac{\overline{v'\rho_v'}}{\overline{\rho}_v}\right) + (1+2.64\overline{\chi}_v+1.32\overline{\chi}_v^2)\frac{\overline{v'p_a'}}{\overline{p}_a}\right]$

2021) are used to give a quantitative example of the errors present in the original equations. When conducting the following quantitative estimations with these data, the vertical components of the equations are used to represent the theoretical 3D equations. This is because the vertical components are of major concerns among the flux community (for example Burns et al. 2021).

This GLEES dataset contains half-hourly covariances between the vertical wind speed and the sonic temperature ($\overline{w'T_s'}$), the water vapor ($\overline{w'\rho_v'}$) and the static air pressure ($\overline{w'p_a'}$) from April 1st, 2018 to September 30th, 2020 (43,872 data for each variable; one datum every half-hour). It also contains half-hourly mean values of water vapor mole fraction ($\overline{\chi}_v$), sonic temperature ($\overline{T}_s$), water vapor density ($\overline{\rho}_v$), ambient air pressure ($\overline{p}_a$) and air temperature ($\overline{T}_a$) for the same period.

Fig. 1 provides an overview of the seasonal variations and frequency distributions of the major variables that will be used in the following analyses, namely $\overline{w'T_s'}/\overline{T}_s$, $\overline{w'\rho_v'}/\overline{\rho}_v$, $\overline{w'p_a'}/\overline{p}_a$ and $\overline{\chi}_v$. Note that the data of complete two years (from July 1st, 2018 to June 30th, 2020), rather than the whole dataset, are used for all the histograms showing frequency distributions in this paper. The approximate values of these variables can be estimated from panels (e) to (h) of Fig. 1 as:

$$\frac{\overline{w'T_s'}}{\overline{T}_s} \approx -3 \times 10^{-4}\ \left(m{\cdot}s^{-1}\right) \tag{18a}$$

$$\frac{\overline{w'\rho_v'}}{\overline{\rho}_v} \approx 2 \times 10^{-3}\ \left(m{\cdot}s^{-1}\right) \tag{18b}$$

$$\frac{\overline{w'p_a'}}{\overline{p}_a} \approx -3 \times 10^{-6}\ \left(m{\cdot}s^{-1}\right) \tag{18c}$$

$$\overline{\chi}_v \approx 4 \times 10^{-3}\ (unitless) \tag{18d}$$

4.2. *Errors of Eq. (B.28)*

Eq. (B.28) is the final aim of Eq. (B.24) and (B.25). It quantifies $\overline{v'T_a'}/\overline{T}_a$, which can be directly used to calculate NEE without the need of $\overline{T}_a$ data Eqs. (15) and ((16)). The equation of the absolute error caused by the original version of Eq. (B.28) is listed in Table 2 as:

$$\Delta\left(\frac{\overline{v'T_a'}}{\overline{T}_a}\right) = \frac{0.32\overline{\chi}_v}{(1+1.64\overline{\chi}_v)(1+1.64\overline{\chi}_v+0.32\overline{\chi}_v^2)}\left[-\overline{\chi}_v(1+1.32\overline{\chi}_v)\left(\frac{\overline{v'T_s'}}{\overline{T}_s} + \frac{\overline{v'\rho_v'}}{\overline{\rho}_v}\right) + \left(1+2.64\overline{\chi}_v+1.32\overline{\chi}_v^2\right)\frac{\overline{v'p_a'}}{\overline{p}_a}\right] \tag{19}$$

Fig. 2 shows the seasonal variations of the correct values of $\overline{w'T_a'}/\overline{T}_a$ calculated by our Eq. (15) with the GLEES data (panel (a)), and those of the absolute errors ($\Delta(\overline{w'T_a'}/\overline{T}_a)$) which are caused by the original Eq. (B.28) and calculated from Eq. (19) (panel (b)). While panels (c) and (d) of Fig. 2 present seasonal variations and frequency distributions, respectively, of the relative errors brought by the original Eq. (B.28).

Comparing Figs. 2(a) and 1(a), we can approximately say that $\overline{w'T_a'}/\overline{T}_a \approx \overline{w'T_s'}/\overline{T}_s$, which is consistent with our estimation in Eq. (15c). Fig. 2(b) shows that the absolute errors of the original Eq. (B.28) are mostly negative when estimating with the GLEES dataset. And we can see from Fig. 2(d) that the relative errors of Eq. (B.28) (compared to its correct version, Eq. (15)) are within the magnitudes of 0.1% ($\pm 1 \times 10^{-3}$).

Further analyzed in Fig. 3 are the seasonal patterns of the absolute errors of Eq. (B.28), which have been calculated with Eq. (19) and shown in panel (b) of Fig. 2. For ease of programming and analyses, we define the terms in Eq. (19) in the following way:

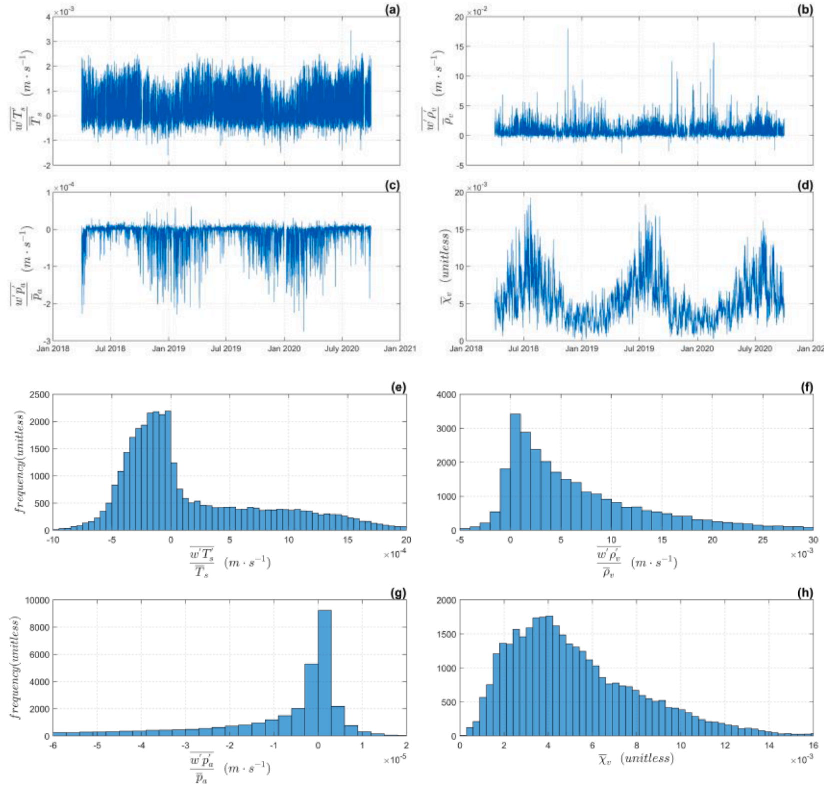

Fig. 1. An overview of the half-hourly mean variables at GLEES to be used in the following quantitative estimations. Panels (a)–(d): seasonal variations of $\overline{w'T_s'}/\overline{T}_s$, $\overline{w'\rho_v'}/\overline{\rho}_v$, $\overline{w'p_a'}/\overline{p}_a$ and $\overline{\chi}_v$, respectively, from April 2018 to September 2020. Panels (e) - (h): Histograms showing the frequency distributions of the same variables, from which the estimations of their magnitudes are derived as Eqs. (18a) – (18d); data from July 1st, 2018 to June 30th, 2020 are used for the histograms hereinafter.

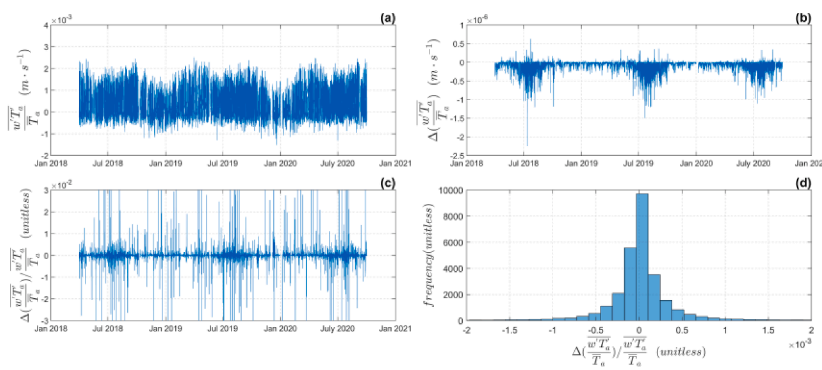

Fig. 2. The values of $\overline{w'T_a'}/\overline{T}_a$ and its absolute and relative errors resulted from the original Eq. (B.28). Panel (a): seasonal variations of the correct values of $\overline{w'T_a'}/\overline{T}_a$ calculated with Eq. (15). Panel (b): seasonal variations of the absolute errors ($\Delta(\overline{w'T_a'}/\overline{T}_a)$) in the original Eq. (B.28) calculated from Eq. (19). Panels (c) and (d): seasonal variations and frequency distributions, respectively, of the relative errors, $\Delta\left(\frac{\overline{w'T_a'}}{\overline{T}_a}\right)\Big/\frac{\overline{w'T_a'}}{\overline{T}_a}$, caused by the original Eq. (B.28).

$$\mathrm{E}_{\chi_v} = \frac{0.32\overline{\chi}_v}{(1+1.64\overline{\chi}_v)\left(1+1.64\overline{\chi}_v+0.32\overline{\chi}_v^2\right)} \tag{19a}$$

$$\mathrm{E}_{T_s} = -\overline{\chi}_v(1+1.32\overline{\chi}_v)\frac{\overline{v'T_s'}}{\overline{T}_s} \tag{19b}$$

$$\mathrm{E}_{v} = -\overline{\chi}_v(1+1.32\overline{\chi}_v)\frac{\overline{v'\rho_v'}}{\overline{\rho}_v} \tag{19c}$$

$$\mathrm{E}_{p} = \left(1+2.64\overline{\chi}_v+1.32\overline{\chi}_v^2\right)\frac{\overline{v'p_a'}}{\overline{p}_a} \tag{19d}$$

Then, Eq. (19) is equivalently rewritten in a more concise way as Eq. (19e) below:

$$\Delta\left(\frac{\overline{v'T_a'}}{\overline{T}_a}\right) = \mathrm{E}_{\chi_v}\left(\mathrm{E}_{T_s}+\mathrm{E}_v+\mathrm{E}_p\right) \tag{19e}$$

Fig. 3 illustrates the magnitude of the vertical component of each term in Eq. (19e). It shows that the T_s term (E_{T_s}) is very small, while the ρ_v and p_a terms are much larger. The ρ_v term (E_v) dominates in summer, while the p_a term (E_p) peaks in winter with a similar magnitude and identical sign. However, the values of parameter E_{χ_v} during summer are approximately four times larger than its values during winter, so the results obtained via solving Eqs. (19) or (19e) do not display notable peaks in winter (Fig. 2(b)).

Diurnal variations of these errors may also be of interest. Fig. 4 provides the seasonal mean diurnal variations for $\overline{w'T_a'}/\overline{T}_a$ (the first

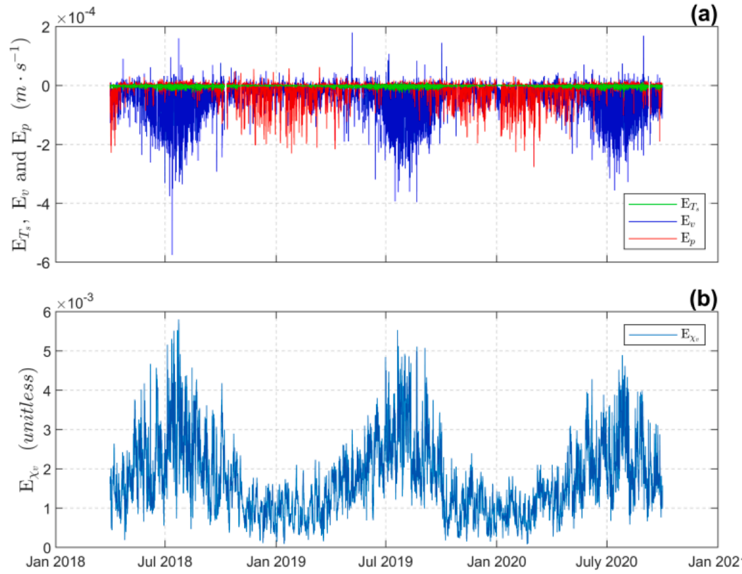

Fig. 3. Seasonal variations of the vertical component of each term in Eq. (19e). These terms help to explain the seasonal patterns of $\Delta(\overline{w'T_a'}/\overline{T}_a)$ which have been calculated by Eq. (19) and shown in Fig. 2(b).

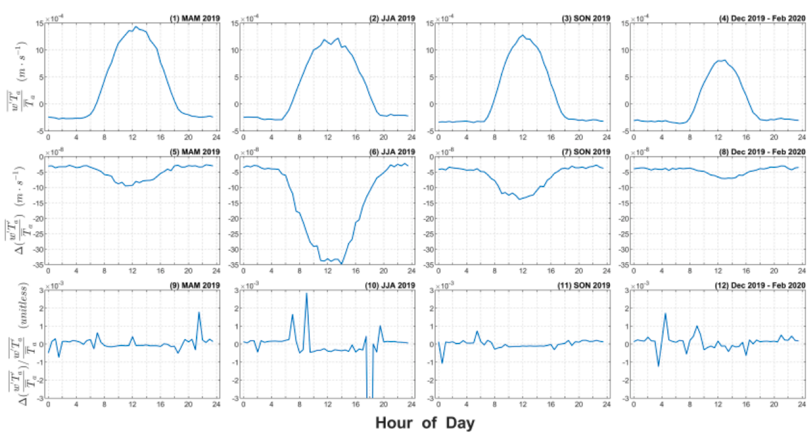

Fig. 4. Seasonal mean diurnal variations of $\overline{w'T_a'}/\overline{T}_a$ (panels (1)-(4)), its absolute error, $\Delta(\overline{w'T_a'}/\overline{T}_a)$ (panels (5)-(8)), and its relative error, $\Delta\left(\frac{\overline{w'T_a'}}{\overline{T}_a}\right)/\frac{\overline{w'T_a'}}{\overline{T}_a}$ (panels (9)-(12)) (MAM: March, April and May. JJA: June, July and August. SON: September, October and November).

row), its absolute error (the second row) and its relative error (the third row) for the year 2019.

In every season, $\overline{w'T_a'}/\overline{T}_a$ peaks at noon with positive values and falls slightly below zero at night, similar to the diurnal patterns of the kinetic sensible heat fluxes ($\overline{w'T_a'}$, not shown). The magnitude of the peak is largest in spring and smallest in winter.

For the absolute error, $\Delta(\overline{w'T_a'}/\overline{T}_a)$, the mean diurnal values are negative all over the year with single peaks at noon (panels (5)-(8) in Fig. 4). The amplitude of the peak is maximum in summer, decreases in fall and reaches the smallest magnitudes in winter. In contrast, the relative error (panels (9)–(12) in Fig. 4), $\Delta\left(\frac{\overline{w'T_a'}}{\overline{T}_a}\right)/\frac{\overline{w'T_a'}}{\overline{T}_a}$, does not display any similar patterns in the seasonal mean diurnal variations as the $\overline{w'T_a'}/\overline{T}_a$ covariance or its absolute error. For the whole year of 2019, the relative error fluctuates around zero within the magnitudes of $\pm 2 \times 10^{-3}$ with few exceptions in summer.

4.3. Errors of Eq. (B.25)

Some researchers may be interested in determining the temperature-wind covariance ($\overline{v'T_a'}$) rather than the covariance divided by the mean air temperature ($\overline{v'T_a'}/\overline{T}_a$) as Eq. (B.28) calculates. Indeed, the temperature-wind covariance could be directly calculated using Eq. (B.25) in Massman and Lee (2002). However, the original Eq. (B.25) contains errors which have been illustrated and corrected in Section 2.2. Here we compare three different formulations of $\overline{v'T_a'}$ that are involved in Section 2.2.

(1) Eq (B.24$_\mathrm{F}$), “the flux version of Eq. (B.24)” mentioned earlier in Section 2.2. It is generated by using $\overline{v'\rho_v'}$ instead of $\overline{v'\rho_v'}^{\mathrm{F}}$ in the original version of Eq. (B.25). It can be rewritten as a function of $\overline{\chi}_v$ in the following equation:

$$\overline{v'T_a'} = \frac{1+\overline{\chi}_v}{1+1.32\overline{\chi}_v}\overline{v'T_s'} - \frac{0.32\overline{\chi}_v}{1+1.32\overline{\chi}_v}\overline{T}_a\left(\frac{\overline{v'\rho_v'}}{\overline{\rho}_v} - \frac{\overline{v'p_a'}}{\overline{p}_a}\right) \tag{B.24v}$$

(2) The original form of Eq. (B.25) in Massman and Lee (2002). By substituting $\overline{v'\rho_v'}^{\mathrm{F}}$ with raw fluxes as Eq. (12b), we produce a version of Eq. (B.25) that is almost equal to Eq. (B.28), with the

only difference of $1/\overline{T}_a$ (Section 2.3). And it can also be rewritten as a function of $\overline{\chi}_v$:

$$\overline{v'T'_a} = \frac{1+\overline{\chi}_v}{1+1.64\overline{\chi}_v+0.32\overline{\chi}_v^2}\overline{v'T'_s} - \frac{0.32\overline{\chi}_v(1+\overline{\chi}_v)}{1+1.64\overline{\chi}_v+0.32\overline{\chi}_v^2}\overline{T}_a\frac{\overline{v'\rho'_v}}{\overline{\rho}_v} + \frac{0.32\overline{\chi}_v(2+\overline{\chi}_v)}{1+1.64\overline{\chi}_v+0.32\overline{\chi}_v^2}\overline{T}_a\frac{\overline{v'p'_a}}{\overline{p}_a} \tag{B.25v}$$

(3) Eq. (13) that we derived in *Section 2.2*, which is the correct version of Eq. (B.25). This can also be expressed as a function of $\overline{\chi}_v$:

$$\overline{v'T'_a} = \frac{1+\overline{\chi}_v}{1+1.64\overline{\chi}_v}\overline{v'T'_s} - \frac{0.32\overline{\chi}_v}{1+1.64\overline{\chi}_v}\overline{T}_a\left(\frac{\overline{v'\rho'_v}}{\overline{\rho}_v} - \frac{\overline{v'p'_a}}{\overline{p}_a}\right) \tag{13v}$$

The absolute errors of Eqs. $(\mathrm{B.24_v})$ and $(\mathrm{B.25_v})$ are calculated as follows by equation sets (20) and (21), respectively:

(1) $(\mathrm{B.24_v}) - (\mathrm{13_v})$:

$$\Delta\left(\overline{v'T'_a}\right) = \frac{0.32\overline{\chi}_v}{(1+1.32\overline{\chi}_v)(1+1.64\overline{\chi}_v)}\left[(1+\overline{\chi}_v)\overline{v'T'_s} - 0.32\overline{\chi}_v\overline{T}_a\left(\frac{\overline{v'\rho'_v}}{\overline{\rho}_v} - \frac{\overline{v'p'_a}}{\overline{p}_a}\right)\right] \tag{20}$$

For simplicity, we define the following terms:

$$\mathrm{C}_{\chi_v} = \frac{0.32\overline{\chi}_v}{(1+1.32\overline{\chi}_v)(1+1.64\overline{\chi}_v)} \tag{20a}$$

$$\mathrm{C}_{T_s} = (1+\overline{\chi}_v)\overline{v'T'_s} \tag{20b}$$

$$\mathrm{C}_v = -0.32\overline{\chi}_v\overline{T}_a\frac{\overline{v'\rho'_v}}{\overline{\rho}_v} \tag{20c}$$

$$\mathrm{C}_p = 0.32\overline{\chi}_v\overline{T}_a\frac{\overline{v'p'_a}}{\overline{p}_a} \tag{20d}$$

Then we can express Eq. (20) equivalently in the following way:

$$\Delta\left(\overline{v'T'_a}\right) = \mathrm{C}_{\chi_v}\left(\mathrm{C}_{T_s} + \mathrm{C}_v + \mathrm{C}_p\right) \tag{20e}$$

If we consider that $\overline{\chi}_v \sim 10^{-3}$ as Eq. (18d), then:

$$\Delta\left(\overline{v'T'_a}\right) \approx 0.32\overline{\chi}_v\cdot\overline{v'T'_s} - (0.32\overline{\chi}_v)^2\cdot\overline{T}_a\cdot\frac{\overline{v'\rho'_v}}{\overline{\rho}_v} + (0.32\overline{\chi}_v)^2\cdot\overline{T}_a\cdot\frac{\overline{v'p'_a}}{\overline{p}_a} \tag{20f}$$

(2) $(\mathrm{B.25_v}) - (\mathrm{13_v})$:

$$\Delta\left(\overline{v'T'_a}\right) = \frac{0.32\overline{\chi}_v}{(1+1.64\overline{\chi}_v)\left(1+1.64\overline{\chi}_v+0.32\overline{\chi}_v^2\right)} \cdot\left[-\overline{\chi}_v(1+\overline{\chi}_v)\overline{v'T'_s} - \overline{\chi}_v(1+1.32\overline{\chi}_v)\overline{T}_a\frac{\overline{v'\rho'_v}}{\overline{\rho}_v} + \left(1+2.64\overline{\chi}_v+1.32\overline{\chi}_v^2\right)\overline{T}_a\frac{\overline{v'p'_a}}{\overline{p}_a}\right] \tag{21}$$

Similarly, we define the following terms:

$$\mathrm{D}_{\chi_v} = \frac{0.32\overline{\chi}_v}{(1+1.64\overline{\chi}_v)\left(1+1.64\overline{\chi}_v+0.32\overline{\chi}_v^2\right)} \tag{21a}$$

$$\mathrm{D}_{T_s} = -\overline{\chi}_v(1+\overline{\chi}_v)\overline{v'T'_s} \tag{21b}$$

$$\mathrm{D}_v = -\overline{\chi}_v(1+1.32\overline{\chi}_v)\overline{T}_a\frac{\overline{v'\rho'_v}}{\overline{\rho}_v} \tag{21c}$$

$$\mathrm{D}_p = \left(1+2.64\overline{\chi}_v+1.32\overline{\chi}_v^2\right)\overline{T}_a\frac{\overline{v'p'_a}}{\overline{p}_a} \tag{21d}$$

and rewrite Eq. (21) as:

$$\Delta\left(\overline{v'T'_a}\right) = \mathrm{D}_{\chi_v}\left(\mathrm{D}_{T_s} + \mathrm{D}_v + \mathrm{D}_p\right) \tag{21e}$$

Still considering $\overline{\chi}_v \sim 10^{-3}$ for approximation, we get:

$$\Delta\left(\overline{v'T'_a}\right) \approx -0.32\overline{\chi}_v^2\cdot\overline{v'T'_s} - 0.32\overline{\chi}_v^2\cdot\overline{T}_a\cdot\frac{\overline{v'\rho'_v}}{\overline{\rho}_v} + 0.32\overline{\chi}_v\cdot\overline{T}_a\cdot\frac{\overline{v'p'_a}}{\overline{p}_a} \tag{21f}$$

Fig. 5 presents the seasonal variations of the correct version of $\overline{w'T'_a}$ calculated by Eq. (13) (panel (a)), and its absolute errors, $\Delta(\overline{w'T'_a})$, caused by Eqs. $(\mathrm{B.24_F})$ and (B.25) and calculated from Eqs. (20) and (21), respectively (panel (b)). Frequency distributions of Eqs. (20) and (21) are shown by histograms in panels (c) and (d), respectively. Fig. 5 (b) shows that while Eq. (B.25) has a smaller magnitude of errors than Eq. $(\mathrm{B.24_F})$ in the quantitative estimations with GLEES data, it contains one additional source of error in formula $(\overline{v'\rho'_v})^{\mathrm{F}}$ instead of $\overline{v'\rho'_v}$, see *Section 2.2* for details). It means that the error of replacing $\overline{v'\rho'_v}$ with $\overline{v'\rho'_v}^{\mathrm{F}}$ in Eq. (B.25) partly cancels out the error of mistaking p_v for ρ_v in Eq. $(\mathrm{B.24_F})$ (see *Section 2.2* or Table 1 for details).

Fig. 6 denotes the dominant terms in the vertical components of Eqs. (20) and (21). The T_s term (C_{T_s}) dominates the errors calculated by Eq. (20) (Fig. 6(a)). However, for Eq. (21), the T_s term (D_{T_s}) is very small; instead, the ρ_v and p_a terms have a much greater magnitude and the same sign (Fig. 6(b)). Fig. 6(b) and Fig. 3(a) are similar because Eqs. (B.25) and (B.28) are almost equivalent (Section 2.3).

We can further explain the results in Figs. 5 and 6 with the approximate magnitudes of the $\overline{w'T'_s}/\overline{T}_s$, $\overline{w'\rho'_v}/\overline{\rho}_v$, $\overline{w'p'_a}/\overline{p}_a$ covariances and $\overline{\chi}_v$ at this site, as shown in Fig. 1 and Eqs. (18a)–(18d).

Eq. (20f), which is a close approximation of Eq. (20), can be further estimated as below:

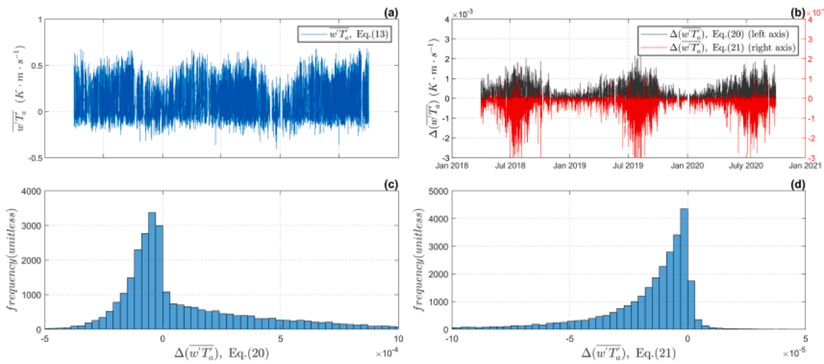

Fig. 5. Seasonal variations of the correct values of $\overline{w'T_a'}$ and its absolute errors, $\Delta(\overline{w'T_a'})$; frequency distributions for the latter. Panel (a): the correct values of $\overline{w'T_a'}$ calculated by Eq. (13). Panel (b): $\Delta(\overline{w'T_a'})$ caused by Eq. (B.24$_F$) (black line, left axis; calculated with Eq. (20)) and Eq. (B.25) (red line, right axis; calculated with Eq. (21)), respectively; note the scale difference between the two y-axes. Panels (c) and (d): histograms showing frequency distributions of Eqs. (20) and (21), respectively.

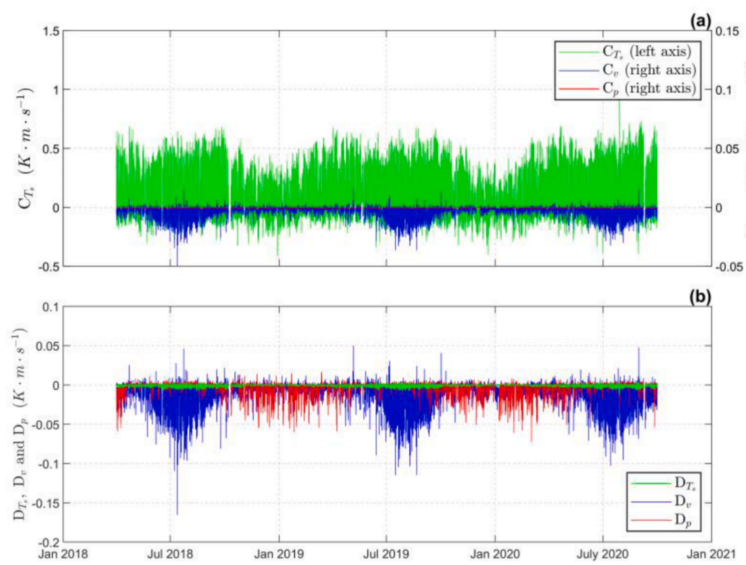

Fig. 6. Seasonal variations of the major terms in Eqs. (20) and (21) (vertical components only). Panel (a): C_{T_s}, C_v and C_p in Eq. (20e); note the scale difference between the two y-axes. Panel (b): D_{T_s}, D_v and D_p in Eq. (21e).

$$0.32\overline{\chi}_v \cdot \overline{w'T_s'} \approx 0.32\overline{\chi}_v \cdot \overline{T}_a \cdot \frac{\overline{w'T_s'}}{\overline{T}_s} \approx 0.32 \times \left(4 \times 10^{-3}\right) \times 300 \times \left(-3 \times 10^{-4}\right) \approx -1 \times 10^{-4} \left(K \cdot m \cdot s^{-1}\right) \tag{22a}$$

$$-(0.32\overline{\chi}_v)^2 \cdot \overline{T}_a \cdot \frac{\overline{w'\rho_v'}}{\overline{\rho}_v} \approx -\left(0.32 \times 4 \times 10^{-3}\right)^2 \times 300 \times \left(2 \times 10^{-3}\right) \approx -1 \times 10^{-6} \left(K \cdot m \cdot s^{-1}\right) \tag{22b}$$

$$(0.32\overline{\chi}_v)^2 \cdot \overline{T}_a \cdot \frac{\overline{w'p_a'}}{\overline{p}_a} \approx \left(0.32 \times 4 \times 10^{-3}\right)^2 \times 300 \times \left(-3 \times 10^{-6}\right) \approx -1 \times 10^{-9} \left(K \cdot m \cdot s^{-1}\right) \tag{22c}$$

Eqs. (22a)–(22c) explain why the T_s term (C_{T_s}) dominates in Eq. (20), as shown in Fig. 6(a). Also demonstrated is the approximate value of Eq. (20) shown in Fig. 5(c), as $(-1) \times 10^{-4}$ $(K \cdot m \cdot s^{-1})$.

Similarly, For Eq. (21f):

$$-0.32\overline{\chi}_v^2 \cdot \overline{w'T_s'} \approx -0.32\overline{\chi}_v^2 \cdot \overline{T}_a \cdot \frac{\overline{w'T_s'}}{\overline{T}_s} \approx -0.32 \times \left(4 \times 10^{-3}\right)^2 \times 300 \times \left(-3 \times 10^{-4}\right) \approx 5 \times 10^{-7} \left(K \cdot m \cdot s^{-1}\right) \tag{23a}$$

$$-0.32\overline{\chi}_v^2 \cdot \overline{T}_a \cdot \frac{\overline{w'\rho_v'}}{\overline{\rho}_v} \approx -0.32 \times \left(4 \times 10^{-3}\right)^2 \times 300 \times \left(2 \times 10^{-3}\right) \approx -3 \times 10^{-6} \left(K \cdot m \cdot s^{-1}\right) \tag{23b}$$

$$0.32\overline{\chi}_v \cdot \overline{T}_a \cdot \frac{\overline{w'p_a'}}{\overline{p}_a} \approx 0.32 \times \left(4 \times 10^{-3}\right) \times 300 \times \left(-3 \times 10^{-6}\right) \approx -1 \times 10^{-6} \left(K \cdot m \cdot s^{-1}\right) \tag{23c}$$

Based on Eqs. (23a)–(23c), the T_s term can be ignored in Eq. (21) as shown in Fig. 6(b). And the values of Eq. (21) can be estimated as $[-3, -1] \times 10^{-6}$ $(K \cdot m \cdot s^{-1})$, which is demonstrated by Eqs. (23b) and (23c) and shown in Fig. 5(d). It is smaller than the magnitude of Eq. (20) by one to two orders, which corresponds with Fig. 5(b).

Despite what is noted above, the values of $\overline{w'T_s'}/\overline{T}_s$, $\overline{w'\rho_v'}/\overline{\rho}_v$, $\overline{w'p_a'}/\overline{p}_a$ and $\overline{\chi}_v$ may not be equal among different sites. Thus, independent estimations are recommended for other sites if one wants to determine the magnitudes and dominant terms of the errors in the temperature-wind covariance brought by the original Eq. (B.25).

5. Conclusions

This paper corrects the typographical error in Eq. (B.24), and the resulting mathematical and logic errors in Eqs. (B.25) and (B.28), which were presented by Massman and Lee (2002). The purpose of these equations was to calculate the air temperature-wind covariance $(\overline{v'T_a'})$

with the directly measured sonic temperature-wind covariance ($\overline{v'T_s'}$), raw water vapor flux ($\overline{v'\rho_v'}$), and pressure-wind covariance ($\overline{v'p_a'}$). We present detailed derivations of the correct equations and the absolute errors brought by the original versions. These theoretical results are sequentially listed in the main text, and summarized in Tables 1 and 2.

Quantitative estimations discussed in Section 4 are achieved using a dataset obtained at GLEES. We present seasonal and mean diurnal variations and frequency distributions of the absolute and relative errors brought by the original Eq. (B.28) to the $\overline{w'T_a'}/\overline{T}_a$ covariance. Our result shows that when the original Eq. (B.28) is used to estimate $\overline{w'T_a'}/\overline{T}_a$, errors are produced with a magnitude of 0.1% of the covariance itself, which is very small. We subsequently present quantitative discussions of all three versions of Eq. (B.25) that calculate the temperature-wind covariance ($\overline{v'T_a'}$). By analyzing the magnitudes of the major variables at GLEES, we explain the magnitudes and dominant terms of the errors when calculating $\overline{w'T_a'}$ with Eqs. (B.24$_F$) and (B.25).

Declaration of Competing Interest

The authors declare that they have no known competing financial interests or personal relationships that could have appeared to influence the work reported in this paper.

Data availability

Data will be made available on request.

Acknowledgments

This research was supported by the National Natural Science Foundation of China (Grant Nos. 91837208) and Strategic Priority Research Program of the Chinese Academy of Sciences (XDA20060101). The authors would like to thank the two anonymous reviewers for their comments which helped to improve this paper substantially.

Appendix: the equivalence of the first-order Reynolds decomposition and first-order Taylor expansion

When deriving Eqs. (3) and (4) from Eq. (2), we truncated the Reynolds decomposition to the first-order, as we have pointed out in *Section 2.1*. The covariance term ($\overline{\sigma'_v p'_a}$) and the second-order fluctuation term ($\sigma'_v p'_a/\overline{\sigma}_v\overline{p}_a$) are ignored in this Reynolds decomposition process, which arrives at the same results of the "first-order Taylor expansion". To make this equivalence clearer, we will present detailed derivations from Eq. (2) to Eqs. (3) and (4) in this Appendix using the first-order Reynolds decomposition and Taylor expansion, respectively.

We start from Eq. (2):

$$\sigma_v \overset{\text{def}}{=} 0.32\frac{p_v}{p_a} \tag{2}$$

(1) To use the rigorous Reynolds decomposition rules and remaining to the first order, we firstly rewrite Eq. (2) equivalently as:

$$\sigma_v p_a = 0.32 p_v \tag{A1}$$

Then applying Reynolds decomposition:

$$\left(\overline{\sigma}_v + \sigma'_v\right)\left(\overline{p}_a + p'_a\right) = 0.32\left(\overline{p}_v + p'_v\right) \tag{A2}$$

Eq. (A2) after Reynolds averaging arrives at:

$$\overline{\sigma}_v\overline{p}_a + \overline{\sigma'_v p'_a} = 0.32\overline{p}_v \tag{A3}$$

Subtracting Eq. (A3) from Eq. (A2), and dividing the result with $\overline{\sigma}_v\overline{p}_a$, we get

$$\frac{\sigma'_v}{\overline{\sigma}_v} = 0.32\frac{p'_a}{\overline{\sigma}_v\overline{p}_a} - \frac{p'_a}{\overline{p}_a} - \frac{\sigma'_v p'_a - \overline{\sigma'_v p'_a}}{\overline{\sigma}_v\overline{p}_a} \tag{A4}$$

Thus, we arrive at the mean and fluctuating values of σ_v. $\overline{\sigma}_v$ is derived from Eq. (A3) rigorously as:

$$\overline{\sigma}_v = 0.32\frac{\overline{p}_v}{\overline{p}_a} - \frac{\overline{\sigma'_v p'_a}}{\overline{p}_a} \tag{A5}$$

and the equation of σ'_v that is similar to Eq. (4), as:

$$\frac{\sigma'_v}{\overline{\sigma}_v} = 0.32\frac{p'_v}{0.32\overline{p}_v - \overline{\sigma'_v p'_a}} - \frac{p'_a}{\overline{p}_a} - \frac{\sigma'_v p'_a - \overline{\sigma'_v p'_a}}{\overline{\sigma}_v\overline{p}_a} \tag{A6}$$

If we ignore the covariance term ($\overline{\sigma'_v p'_a}$) and the second-order fluctuation term ($\sigma'_v p'_a/\overline{\sigma}_v\overline{p}_a$) in Eqs. (A5) and A6), then we get Eqs. (3) and ((4) in the main text:

$$\overline{\sigma}_v = 0.32\frac{\overline{p}_v}{\overline{p}_a} \tag{3}$$

$$\frac{\sigma'_v}{\overline{\sigma}_v} = \frac{p'_v}{\overline{p}_v} - \frac{p'_a}{\overline{p}_a} \tag{4}$$

(2) Using the "first-order Taylor expansion":

The first-order Tayler expansion includes the zero-order Taylor expansion, which means:

$$\sigma_v(x_0) \stackrel{\text{def}}{=} 0.32\frac{p_v(x_0)}{p_a(x_0)} \tag{A7}$$

where x_0 is the "base point" in Taylor expansion. If we regard the mean values of the above variables as their values of the x_0 point, then we get Eq. (3).

To get the first-order expansion, we firstly apply logarithm to Eq. (2) as:

$$\ln\sigma_v = \ln p_v - \ln p_a + \ln 0.32 \tag{A8}$$

Then conducting the first-order derivative, we get

$$\frac{d\sigma_v}{\overline{\sigma}_v} = \frac{dp_v}{\overline{p}_v} - \frac{dp_a}{\overline{p}_a} \tag{A9}$$

And if we regard the fluctuations of the three variables above (σ_v', p_v' and p_a') to be small enough, then we can replace the differential terms in the numerators with the fluctuations, just as Eq. (4).

Thus, the first-order Reynolds decomposition and Taylor expansion arrive at the same results, which means they are equivalent.

References

Burba, G., 2022. Eddy Covariance Method for Scientific, Regulatory, and Commercial Applications. LI-COR Biosciences.

Burns, S.P., Frank, J.M., Massman, W.J., Patton, E.G., Blanken, P.D., 2021. The effect of static pressure-wind covariance on vertical carbon dioxide exchange at a windy subalpine forest site. Agric. For. Meteorol. 306, 108402 https://doi.org/10.1016/j.agrformet.2021.108402. ISSN 0168-1923.

Frank, J.M., Massman, W.J., 2021. AmeriFlux BASE US-GLE GLEES, Ver. 8-5. AmeriFlux AMP (Dataset). https://doi.org/10.17190/AMF/1246056.

Fuehrer, P.L., Friehe, C.A., 2002. Flux corrections revisited. Bound. Layer Meteorol. 102, 415–457. https://doi.org/10.1023/A:1013826900579.

Gu, L., Massman, W.J., Leuning, R., Pallardy, S.G., Meyers, T., Hanson, P.J., Riggs, J.S., Hosman, K.P., Yang, B., 2012. The fundamental equation of eddy covariance and its application in flux measurements. Agric. For. Meteorol. 152, 135–148. https://doi.org/10.1016/j.agrformet.2011.09.014. VolumePagesISSN 0168-1923.

Kowalski, A.S., Serrano-Ortiz, P., Miranda-García, G., Fratini, G., 2021. Disentangling turbulent gas diffusion from non-diffusive transport in the boundary layer. Bound. Layer Meteorol. 179 (3), 347–367. https://doi.org/10.1007/s10546-021-00605-5.

Lee, X., Massman, W.J., 2011. A perspective on thirty years of the webb, pearman and leuning density corrections. Bound. Layer Meteorol. 139, 37–59. https://doi.org/10.1007/s10546-010-9575-z.

Leuning, R., Lee, X., Massman, W., Law, B., 2004. Measurements of trace gas fluxes in the atmosphere using eddy covariance: WPL corrections revisited. In: Handbook of Micrometeorology. Atmospheric and Oceanographic Sciences Library, eds, 29. Springer, Dordrecht. https://doi.org/10.1007/1-4020-2265-4_6.

Leuning, R., 2007. The correct form of the Webb, Pearman and Leuning equation for eddy fluxes of trace gases in steady and non-steady state, horizontally homogeneous flows. Bound. Layer Meteorol. 123, 263–267. https://doi.org/10.1007/s10546-006-9138-5.

Massman, W.J., Lee, X., 2002. Eddy covariance flux corrections and uncertainties in long-term studies of carbon and energy exchanges. Agric. For. Meteorol. 113 (1–4), 121–144. https://doi.org/10.1016/S0168-1923(02)00105-3. IssuesISSN 0168-1923.

Paw U, K.T., Baldocchi, D.D., Meyers, T.P., Wilson, K.B., 2000. Correction of eddy-covariance measurements incorporating both advective effects and density fluxes. Bound. Layer Meteorol. 97, 487–511. https://doi.org/10.1023/A:1002786702909.

Webb, E.K., Pearman, G.I., Leuning, R., 1980. Correction of flux measurements for density effects due to heat and water vapor transfer. Q. J. R. Meteorol. Soc. 106, 85–100. https://doi.org/10.1002/qj.49710644707.